Intramicellar Glass Transition and Liquid Dynamics in Soft Confinement

Li-Min Wang, Fang He, and Ranko Richert

Department of Chemistry and Biochemistry, Arizona State University, Tempe, Arizona 85287-1604, USA
(Received 19 November 2003; published 3 March 2004)

We explore the dynamics of viscous propylene glycol (PG) near its glass transition for the case of soft spatial confinement. The supercooled liquid is geometrically restricted by the reverse micelles of a glass-forming PG/AOT/decalin microemulsion, with the intramicellar dynamics being probed by triplet state solvation dynamics. While hard confinement by porous solids is known to result in slower dynamics and an increased glass transition temperature T_g of PG, the nanodroplets suspended in a more fluid environment display faster structural relaxation, equivalent to a reduction of T_g as observed in freestanding polymer films.

The increasing demand of materials which are required to perform on spatial scales as small as several nanometers challenges our understanding of how geometrical confinement and interfacial situations change the properties of condensed matter [1]. Finite size and boundary effects are important in the context of microlubrication [2–4], the retrieval and transport of liquids in porous rocks, and the mobility of matter in cells and membranes. Interest in nanometer confinement also arises from the prospect of advancing our knowledge in the field of glass-forming liquids, i.e., disordered materials in their highly viscous liquid state near the glass transition temperature T_g [5,6]. Because the sluggish dynamics of highly supercooled liquids are associated with inherent length scales of several nanometers [7,8], these liquids are particularly sensitive to finite size and surface effects.

Porous silica glasses have been employed extensively in order to study the behavior of liquids in restricting geometries [9–12]. Jackson and McKenna have discovered that nanometer scale geometrical confinement affects the calorimetric T_g of molecular glass-forming materials [13]. Many other techniques have been applied in order to quantify how confinement changes the behavior of supercooled liquids and polymers [14–18], but a generally accepted understanding is still lacking. With the exception of freestanding polymer film studies [19], confinement is always realized by solid boundaries which often act as an additional barrier to structural relaxation. The aim of this work is to explore the consequences of soft confinement, where a supercooled molecular liquid droplet is surrounded by a rapidly fluctuating rather than static environment.

The present approach to soft confinement is based upon the capability of selected glass-forming compounds to self-assemble as microemulsions [20–22]. In order to detect the structural relaxation within the droplets with the optical technique of solvation dynamics, we focus on reverse micelles, i.e., microemulsions of the "water-in-oil" type. The first such system with extended low-temperature stability based upon glass-forming components has been reported and characterized by Green [23]. For the present purpose, we have focused on three component systems using propylene glycol (PG, 1,2-propanediol) as the polar or "water" phase and decalin (DHN, decahydro-naphthalene) as the nonpolar or "oil" phase. In the absence of a surfactant, PG and DHN are virtually immiscible. The respective glass transition temperatures of the bulk liquids are $T_g = 167$ K for PG and $T_g = 135$ K for DHN. As a surfactant for reverse micelles, we chose AOT [aerosol OT, sodium bis(2-ethylhexyl)sulfosuccinate] [24]. Using the techniques established previously [20], we have identified the regime of stable and optically clear microemulsions within the phase diagram of this ternary system shown in Fig. 1. Within the area of stability at 25 °C, a range has been found in which the samples remain stable also during cooling to 77 K, where both the polar and nonpolar phases are in their vitreous state below T_g. The sample used for the subsequent dynamics study has the following composition: 10.2% PG, 36.1% AOT, and 53.7% DHN (by weight).

The average size of the present PG nanodroplets is estimated on the basis of the volumetric composition. Assuming spherical reverse micelles of uniform size and using the reported thickness of the AOT surfactant layer of $r = 1.33$ nm [24], the radius R of the PG droplet and the volume ratio are related by

$$\frac{V_{AOT}}{V_{PG}} = \frac{\frac{4}{3}\pi[(R+r)^3 - R^3]}{\frac{4}{3}\pi R^3} = \left(1 + \frac{r}{R}\right) - 1. \quad (1)$$

The present composition translates into a volume ratio $V_{AOT}/V_{PG} = 3.0$ for the AOT and PG components, with the amount of the continuous phase DHN defining only the average distance between the reverse micelles. As a result of this calculation, we obtain a diameter for the intramicellar PG of 4.6 nm.

With the above suitable system at hand, we now assess the dynamics of PG confined in these reverse micelles. To this end, the technique of triplet state solvation dynamics
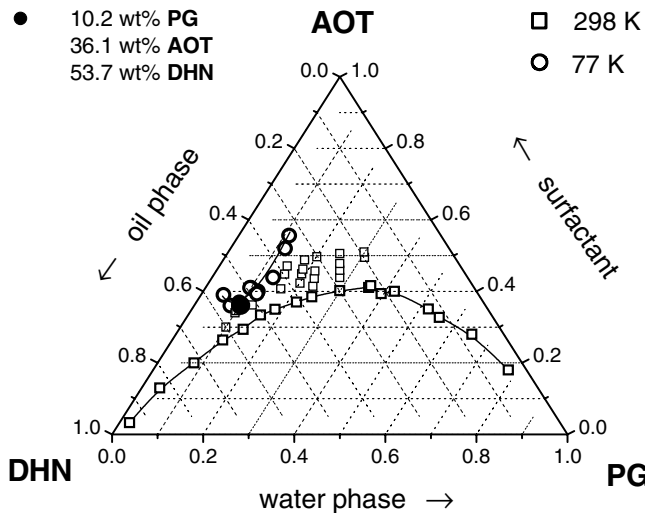
FIG. 1. Phase diagram of the mixture of decalin (DHN, nonpolar oil phase), sodium bis(2-ethylhexyl)sulfosuccinate (AOT, surfactant), and propylene glycol (PG, polar water phase). The lines identify the phase boundaries for microemulsion formation at 298 K (rectangles) and 77 K (circles), respectively. The composition used for the solvation experiments is identified as a solid circle at 10.2% PG, 36.1% AOT, and 53.7% DHN by weight.

is employed, which allows one to observe the relaxation of liquids by optical spectroscopy [25]. The method exploits the change in the permanent dipole moment, $\Delta \vec{\mu} = \vec{\mu}_E - \vec{\mu}_G$, which results from the electronic excitation of the solute molecule and its interaction with the fluctuations of the solvent dipoles. The liquid to be studied is doped with quinoxaline (QX) as chromophore and the time resolved $S_0 \leftarrow T_1(0 - 0)$ emission spectra are recorded and analyzed in order to obtain the average emission energy $\langle \bar{\nu}(t) \rangle$ as a function of time. Normalization according to $\langle \bar{\nu}(t = 0) \rangle \rightarrow 1$ and $\langle \bar{\nu}(t \rightarrow \infty) \rangle \rightarrow 0$ yields the solvation correlation function

$$C(t) = \frac{\langle \bar{\nu}(t) \rangle - \langle \bar{\nu}(\infty) \rangle}{\langle \bar{\nu}(0) \rangle - \langle \bar{\nu}(\infty) \rangle}, \tag{2}$$

which is known to reflect the structural relaxation of the liquid [26]. The amplitude of the observed total redshift $\Delta \bar{\nu} = \langle \bar{\nu}(0) \rangle - \langle \bar{\nu}(\infty) \rangle$ depends strongly on factors such as $\Delta \vec{\mu}$ of the solute and the polarity or static dielectric constant ε_s of the solvent. Solvation techniques have been employed earlier in the study of viscous liquids confined to porous glasses [27,28] and in the context of picosecond dynamics in reverse micelles [29,30].

For the polar liquid PG, we have observed $\Delta \bar{\nu} = 21\,135 \text{ cm}^{-1} - 20\,620 \text{ cm}^{-1} = 515 \text{ cm}^{-1}$, whereas the nonpolar liquid DHN displays a redshift as small as $\Delta \bar{\nu} = 30 \text{ cm}^{-1}$ [31]. These values refer to the bulk liquids near their respective T_g. This difference in $\Delta \bar{\nu}$ helps in identifying the spatial origin of the QX emission, intramicellar (PG) versus continuous phase (DHN). Near $T =$

170 K, the emission of the microemulsion sample displays a total energy shift of $\Delta \bar{\nu} = 510 \text{ cm}^{-1}$, corresponding to the value of bulk PG. Additionally, this emission is observed approximately 30 K above the $T_g = 135$ K of DHN, where oxygen diffusion is sufficiently fast to quench any residual triplet states within the continuous DHN phase. Therefore, the present solvation experiments specifically probe the dynamics of the intramicellar PG. The solvation experiments were performed with anhydrous versus air-exposed AOT, with the result that the 4 wt. % H_2O uptake of the surfactant has no detectable effect on the dynamics of the intramicellar PG. Additionally, systematic differences in the solvation $C(t)$ data for bulk PG as pure liquid and after saturration with DHN remained absent. We conclude that the intramicellar PG is not being plasticized by H_2O or DHN uptake within the microemulsion.

The prominent features of supercooled liquids are the complex behavior regarding the time and temperature dependence of their structural α relaxation. At the glass transition temperature T_g, the relaxation time scale associated with viscous flow reaches $\tau_g = 100$ s. Relaxations of glass-forming materials often exhibit a Kohlrausch-Williams-Watts(KWW)–type correlation function,

$$C(t) = \exp[-(t/\tau)^\beta], \tag{3}$$

where the exponent $0 < \beta \leq 1$ quantifies the deviation from an exponential pattern. In the majority of these systems, the temperature dependence $\tau(T)$ obeys the Vogel-Fulcher-Tammann (VFT) expression,

$$\log_{10}(\tau/s) = A + B/(T - T_0). \tag{4}$$

Following common practice, we analyze the solvation dynamics results in terms of the above KWW function in order to quantify the relaxation time by τ and its dispersion by β. For bulk PG, the stretching exponent is $\beta = 0.37$, whereas the intramicellar PG displays a broader distribution of relaxation times, $\beta = 0.25$. Expectedly, the characteristic relaxation times $\tau(T)$ obtained from the solvation experiment on the bulk liquid closely follow the dielectric relaxation times. However, the PG subject to soft confinement relaxes a factor of ≈ 35 faster than its bulk counterpart at the same temperature, $T = 171$ K. Therefore, the intramicellar PG is associated with a lower glass transition, $T_g = 160$ K, and a confinement induced reduction of the glass transition temperature by $\Delta T_g = -7$ K. An activation map of the solvent response time results, $\tau(T)$, is shown as symbols in Fig. 2.

Propylene glycol is an excellent glass former with a substantial dielectric loss. Therefore, the dynamics of this compound has been studied extensively, as a bulk liquid [32] and in confining geometries [16,33–36]. As observed for many other molecular liquids, the dynamics of PG is frustrated as a result of hard confinement to porous silica,
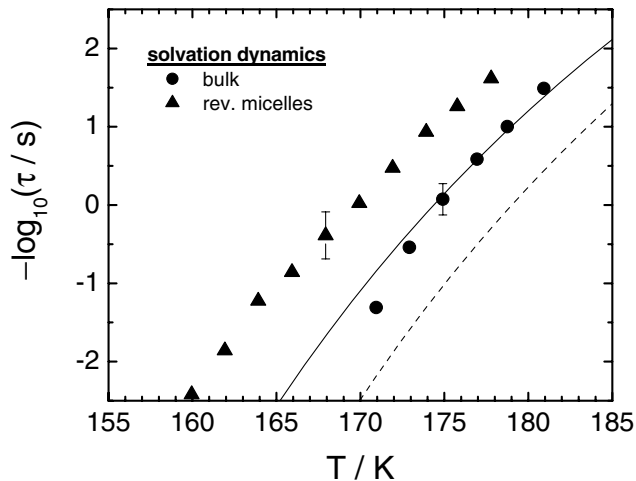
FIG. 2. Characteristic relaxation times τ for propylene glycol as a bulk liquid and subject to different types of confinement. Solid symbols are for the present solvation dynamics results on bulk PG (solid circles) and on PG confined to the 4.6 nm diameter reverse micelles in the PG/AOT/DHN microemulsion. The lines are VFT fits to dielectric relaxation data, $\tau_{max}(T)$, for bulk PG (solid) and for PG confined to porous glass samples with 10 nm pore diameter [16].

corresponding to a positive glass transition shift of $\Delta T_g = +4.5$ K. The activation plot in Fig. 2 includes these dielectric results for bulk PG and for PG confined to controlled porous glass samples with 10 nm pore size [16]. In contrast to the situation of the present microemulsions, confinement to porous silica ($T_g = 1500$ K) involves an interfacial liquid layer in contact with a static wall, which acts as an additional barrier to structural relaxation [37]. That interfacial frustration can dominate the confinement effects is clearly seen in the case of 3-methylpentane confined to porous glass subject to spatially selective probing [38]. In that case, the interfacial relaxation time is a factor of 2000 larger than the bulk value at the same temperature, whereas the effect inside the pore volume amounts to a factor of 40 only. The soft confinement realized in the present microemulsion reverses the situation, because the confined PG droplet is surrounded by a more fluid environment. Hence, it is not unexpected that the dynamics at the AOT boundary is accelerated compared to bulk PG, and the length scale of cooperativity will determine how far the effect will penetrate into the liquid. A more quantitative comparison of the confinement effects of porous glasses and microemulsions needs to account for the geometrical differences as well. As an example, the dimensionality of the confining geometry (two dimensional in the case of cylindrical pores versus three dimensional for spherical droplets) has been demonstrated to change the net effect [39,40].

Because the above-mentioned previous studies of confined PG are based on dielectric relaxation measurements, we have also performed dielectric experiments on the present PG/AOT/DHN microemulsion in order to

facilitate a direct comparison with the case of hard confinement. After subtracting excessive dc conductivity, the dielectric loss spectra $\varepsilon''(\omega)$ reveal peaks positioned at $\tau_{max} = 1/\omega_{max}$, which again indicate accelerated dynamics relative to the bulk PG, as shown in Fig. 3. A further lower frequency loss peak is seen identically in soft and hard confinement (open symbols in Fig. 3), possibly a result of conductivity within the confined PG combined with the Maxwell-Wagner effects inherent in heterogeneous dielectrics. The bottom line of this dielectric experiment is that the qualitative difference between soft and hard confinement effects is not a matter of the experimental technique.

Finally, we compare the present experimental situation and findings to those encountered in the studies of thin freestanding polymer films [19,41]. In such polymer films as thin as 7 nm, the dynamics depend substantially on the presence or absence of a substrate [42]. With respect to the absence of a solid substrate or boundary, a glass-forming microemulsion with an intramicellar T_g above that of the continuous phase is currently the molecular system which is closest to the situation of a free surface or self-supporting polymer film. That both freestanding films and nanodroplets suspended in a fluid show a significant T_g depression could indicate that the features observed for freestanding films are not polymer specific.

In conclusion, we have explored the dynamics of viscous propylene glycol within droplets of 4.6 nm diameter suspended in a more fluid environment. This soft confinement is achieved by the formation of reverse micelles, i.e.,
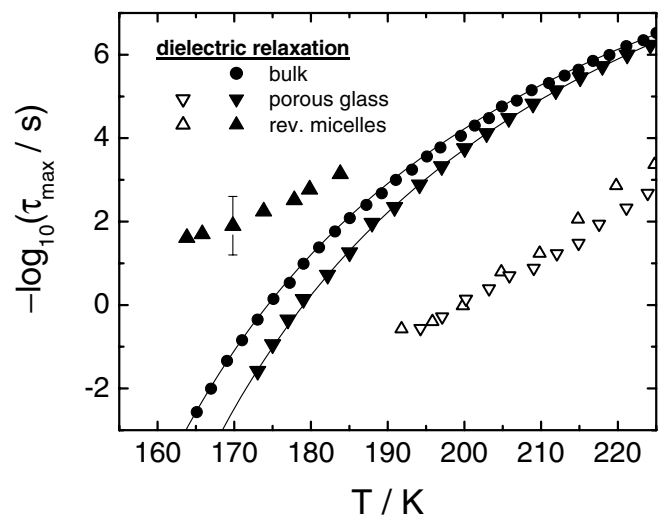

FIG. 3. Dielectric relaxation times τ_{max} for propylene glycol as a bulk liquid (solid circles) and subject to different types of confinement. Triangles pointing up are for PG confined to the 4.6 nm diameter reverse micelles in the PG/AOT/DHN microemulsion, while triangles pointing down are for PG in porous glass samples with 10 nm pore diameter [16]. Solid symbols identify the structural or α relaxation, while open symbols are associated with the effects of dc conductivity in confinement. The lines are VFT fits to the respective $\tau_{max}(T)$ data.

by microemulsions of the water-in-oil type, where PG is the intramicellar compound. Because all components of this ternary system support glass formation, we find a composition range in which the self-assembled structures remain stable near the glass transition of PG at $T_g = 160$ K. Here, we identify soft confinement with the situation in which the T_g of the confining material is below that of the confined substance, whereas hard confinement refers to the inverted relation of the structural relaxation times. The striking result of the present study is that the dynamics of PG in soft confinement is accelerated, whereas the usual hard confinement has always led to frustrated relaxation of PG near its T_g. In the PG nanodroplets, the α relaxation time is approximately 1.5 decades faster than in the bulk, equivalent to a glass transition shift of $\Delta T_g = -7$ K. This dependence on the particular boundary conditions, soft versus hard, suggests that the dynamics of the confining material is a critical factor in determining the net confinement effect. With polymeric materials, the possibility of investigating self-supporting films with free surfaces has led to analogous results if the dynamics at a free surface is compared with those at a solid substrate.

---

[1] T. R. Böhme and J. J. de Pablo, J. Chem. Phys. **116**, 9939 (2002).

[2] R. G. Horn and J. N. Israelachvili, J. Chem. Phys. **75**, 1400 (1981); J. N. Israelachvili and P. M. McGuiggan, Science **241**, 795 (1988).

[3] J. Van Alsten and S. Granick, Phys. Rev. Lett. **61**, 2570 (1988); S. Granick, Science **253**, 1374 (1991).

[4] J. Gao, W. D. Luedtke, and U. Landman, J. Chem. Phys. **106**, 4309 (1997).

[5] M. D. Ediger, C. A. Angell, and S. R. Nagel, J. Phys. Chem. **100**, 13 200 (1996).

[6] C. A. Angell, K. L. Ngai, G. B. McKenna, P. F. McMillan, and S. W. Martin, J. Appl. Phys. **88**, 3113 (2000).

[7] M. D. Ediger, Annu. Rev. Phys. Chem. **51**, 99 (2000).

[8] R. Richert, J. Phys. Condens. Matter **14**, R703 (2002).

[9] J. M. Drake and J. Klafter, Phys. Today **43**, 46 (1990).

[10] *Molecular Dynamics in Restricted Geometries*, edited by J. M. Drake and J. Klafter (Wiley, New York, 1989).

[11] J. Warnock, D. D. Awschalom, and M. W. Shafer, Phys. Rev. B **34**, 475 (1986).

[12] B. J. Loughnane, A. Scodinu, and J. T. Fourkas, J. Phys. Chem. B **103**, 6061 (1999).

[13] C. L. Jackson and G. B. McKenna, J. Non-Cryst. Solids **131–133**, 221 (1991).

[14] J. Zhang, G. Liu, and J. Jonas, J. Phys. Chem. **96**, 3478 (1992).

[15] A. Huwe, F. Kremer, P. Behrens, and W. Schweiger, Phys. Rev. Lett. **82**, 2338 (1999).

[16] J. Schüller, Yu. B. Mel'nichenko, R. Richert, and E. W. Fischer, Phys. Rev. Lett. **73**, 2224 (1994).

[17] G. Barut, P. Pissis, R. Pelster, and G. Nimtz, Phys. Rev. Lett. **80**, 3543 (1998).

[18] H. Wendt and R. Richert, J. Phys. Condens. Matter **11**, A199 (1999).

[19] J. A. Forrest, K. Dalnoki-Veress, J. R. Stevens, and J. R. Dutcher, Phys. Rev. Lett. **77**, 2002 (1996).

[20] C. A. Angell, R. K. Kadiyala, and D. R. MacFarlane, J. Phys. Chem. **88**, 4593 (1984).

[21] J. Dubochet, M. Adrian, J. Teixeira, C. M. Alba, R. K. Kadiyala, D. R. MacFarlane, and C. A. Angell, J. Phys. Chem. **88**, 6727 (1984).

[22] C. Alba-Simionesco, J. Teixeira, and C. A. Angell, J. Chem. Phys. **91**, 395 (1989).

[23] J. L. Green, J. Phys. Chem. **94**, 5647 (1990).

[24] M. Kotlarchyk, S.-H. Chen, J. S. Huang, and M. W. Kim, Phys. Rev. Lett. **53**, 941 (1984).

[25] R. Richert, J. Chem. Phys. **113**, 8404 (2000).

[26] M. Maroncelli and G. R. Fleming, J. Chem. Phys. **86**, 6221 (1987).

[27] C. Streck, Yu. B. Mel'nichenko, and R. Richert, Phys. Rev. B **53**, 5341 (1996).

[28] R. Richert, Phys. Rev. B **54**, 15 762 (1996).

[29] R. E. Riter, E. P. Undiks, J. R. Kimmel, and N. E. Levinger, J. Phys. Chem. B **102**, 7931 (1998).

[30] D. M. Willard, R. E. Riter, and N. E. Levinger, J. Am. Chem. Soc. **120**, 4151 (1998).

[31] M. Yang and R. Richert, Chem. Phys. **284**, 103 (2002).

[32] C. A. Angell and D. L. Smith, J. Phys. Chem. **86**, 3845 (1982).

[33] Yu. B. Mel'nichenko, J. Schüller, R. Richert, B. Ewen, and C.-K. Loong, J. Chem. Phys. **103**, 2016 (1995).

[34] A. Huwe, M. Arndt, F. Kremer, C. Haggenmüller, and P. Behrens, J. Chem. Phys. **107**, 9699 (1997).

[35] W. Gorbatschow, M. Arndt, R. Stannarius, and F. Kremer, Europhys. Lett. **35**, 719 (1996).

[36] G. Carini, V. Crupi, G. D'Angelo, D. Majolino, P. Migliardo, and Yu. B. Mel'nichenko, J. Chem. Phys. **107**, 2292 (1997).

[37] B. J. Loughnane, R. A. Farrer, A. Scodinu, T. Reilly, and J. T. Fourkas, J. Phys. Chem. B **104**, 5421 (2000).

[38] R. Richert and M. Yang, J. Phys. Chem. B **107**, 895 (2003).

[39] G. Barut, P. Pissis, R. Pelster, and G. Nimtz, Phys. Rev. Lett. **80**, 3543 (1998).

[40] P. Pissis, A. Kyritsis, G. Barut, R. Pelster, and G. Nimtz, J. Non-Cryst. Solids **235–237**, 444 (1998).

[41] C. J. Ellison and J. M. Torkelson, Nature Materials **2**, 695 (2003).

[42] J. L. Keddie, R. A. L. Jones, and R. A. Cory, Europhys. Lett. **27**, 59 (1994).